

# PQC-HA: A Framework for Prototyping and In-Hardware Evaluation of Post-Quantum Cryptography Hardware Accelerators <sup>★</sup>

Richard Sattel<sup>[0009-0003-1060-3462]</sup>, Christoph Spang<sup>[0000-0003-1606-4474]</sup>,  
Carsten Heinz<sup>[0000-0001-5927-4426]</sup>, and Andreas Koch<sup>[0000-0002-1164-3082]</sup>

Embedded Systems and Applications Group, TU Darmstadt, Germany  
{sattel, spang, heinz, koch}@esa.tu-darmstadt.de

**Abstract.** In the third round of the NIST Post-Quantum Cryptography standardization project, the focus is on optimizing software and hardware implementations of candidate schemes. The winning schemes are CRYSTALS Kyber and CRYSTALS Dilithium, which serve as a Key Encapsulation Mechanism (KEM) and Digital Signature Algorithm (DSA), respectively. This study utilizes the TaPaSCo open-source framework to create hardware building blocks for both schemes using High-level Synthesis (HLS) from minimally modified ANSI C software reference implementations across all security levels. Additionally, a generic TaPaSCo host runtime application is developed in Rust to verify their functionality through the standard NIST interface, utilizing the corresponding Known Answer Test mechanism on actual hardware. Building on this foundation, the communication overhead for TaPaSCo hardware accelerators on PCIe-connected FPGA devices is evaluated and compared with previous work and optimized AVX2 software reference implementations. The results demonstrate the feasibility of verifying and evaluating the performance of Post-Quantum Cryptography accelerators on real hardware using TaPaSCo. Furthermore, the off-chip accelerator communication overhead of the NIST standard interface is measured, which, on its own, outweighs the execution wall clock time of the optimized software reference implementation of Kyber at Security Level 1.

**Keywords:** Post-Quantum Cryptography · NIST · CRYSTALS Kyber · CRYSTALS Dilithium · FPGA · Hardware Accelerator · High-level Synthesis · TaPaSCo

## 1 Introduction

From the perspective of recent progress in the field of quantum computing, the National Institute of Standards and Technology (NIST) is setting out to

---

<sup>★</sup> This research was funded by the German Federal Ministry for Education and Research (BMBF) with the funding ID 01IS17050. This research work was supported by the National Research Center for Applied Cybersecurity ATHENE. ATHENE is funded jointly by the German Federal Ministry of Education and Research and the Hessian Ministry of Higher Education, Research and the Arts

standardize a set of algorithms for Post-Quantum Cryptography (PQC) to replace the majority of public-key cryptography in use today that will become insecure with the advent of large quantum computers leaving most communication unprotected. The third round of this competition elects CRYSTALS Kyber and CRYSTALS Dilithium as winners, for a Key Encapsulation Mechanism (KEM) and Digital Signature Algorithm (DSA) respectively, with a focus on optimized software and hardware implementations. The Task Parallel System Composer (TaPaSCo) open-source framework provides essential components to aid in the design process of these hardware accelerators, such as a generic hardware architecture in addition to a Linux kernel driver and userspace runtime library, which complement one another to schedule jobs on TaPaSCo Processing Elements (PEs)[8]. In this work, we present the basis for the integration of PQC building blocks into the TaPaSCo framework. We use High-level Synthesis (HLS) to transform the top-level functions of CRYSTALS Kyber and CRYSTALS Dilithium into PEs, which are hardware kernels containing logic to solve a specific task. We synthesize PEs of all NIST security levels for *Encapsulation* and *Decapsulation* for Kyber as well as *Sign* and *Verify* for Dilithium. The PEs receive their parameters from a host runtime application implemented in Rust using the standard NIST interface, which is a set of functions that each candidate of the NIST PQC project needs to implement. It is used to test the functional correctness of the PEs via the NIST Known Answer Test (KAT) cases, which are in turn verified to be correct with upstream repository hashes, to make sure they generate the same results as the correct upstream reference software implementation. To enable verification of algorithms that depend on random input data deterministically and at the same time avoid using insecure Random Number Generator (RNG) units on the Field-programmable Gate Array (FPGA), we extend the NIST interface to supply the PEs with pre-initialized random buffers from the host. The runtime provides generic functions for KEM and DSA algorithms and defines an extendable interface, which facilitates the integration of further algorithms of the NIST PQC project as long as they adhere to the NIST mandatory interface, optionally including the random buffer extension. The rest of this work is organized as follows. In Sect. 2, we discuss related work for HLS and Hardware Description Language (HDL) implementations, which we will later compare to our implementations. In Sect. 3, we define our approach. We describe how we use HLS to create TaPaSCo PEs from the current software ANSI C reference implementation using the same standard interface for parameters. In Sect. 4, we present the results of our designs, compare them to related work and analyze the communication overhead of the chosen interface. Finally, we conclude our work in Sect. 5 and end with subsequent ideas in Sect. 6.

## 2 Related Work

### 2.1 HLS Implementations

In the prior work [1] and the follow-up publication [15], where the authors expand their results for signature schemes but report results only for the Artix-7 platform, Basu *et al.* and Soni *et al.* present the implementation of multiple candidates in round two. They also list updated results of resource usage, clock, and latency in tables on their website [14] and publish some of their Vivado projects on Github [13]. We compare our designs with the results of this work in Sect. 4.

In [16], Zhao *et al.* extend the NIST standard interface with a random buffer to be supplied by the host software application, which is an approach also used in this work. They also present optimized HLS designs for the *Kyber512* variant of CRYSTALS Kyber in round two, which at this point claimed a security Level of 1, and report an improvement of 74.6% for the encapsulation and 54.4% for the decapsulation compared to the prior work in [1] for the Latency-area Product (LAP)  $\times$  clock period metric. We compare our results with this work in Sect. 4.

### 2.2 HDL Implementations

In [5], Dang *et al.* evaluate existing hardware implementations for round three KEM candidates. They make a distinction between *lightweight* and *high-performance* implementations and conclude that HLS implementations are inferior both in resource usage and performance compared to HDL implementations. They present new *high-performance* HDL designs for CRYSTALS Kyber, Saber, and NTRU KEM schemes, which they claim to be the fastest concerning latency to date. We compare our results with this work in Sect. 4.

In [11], Land *et al.* present new *lightweight* FPGA implementations of the CRYSTALS Dilithium DSA scheme, of which they claim to make the most efficient use of resources, surpassing the results of [12]. They also publish their implementations as open-source, which makes them a promising DSA candidate for integration in TaPaSCo. The authors of another *high-performance* Dilithium HDL implementation [3] claim to beat this work in terms of latency but require more resources, which is the reason why we choose this work for comparison with our results in Sect. 4.

### 2.3 TaPaSCo-related Work

In [9], Heinz *et al.* present multiple open-source RISC-V cores made ready to use as TaPaSCo PEs. They evaluate the performance of their designs in hardware utilizing the same Linux kernel driver and runtime libraries as this work. This approach serves as an example, which we are adapting for PQC accelerators. These RISC-V PEs could be extended with in-pipeline PQC accelerators leveraging HDL methodologies as in [7]. On the contrary, communication with other standalone accelerators as presented in this work is not implicitly supported, but requires to implement an individual TaPaSCo interconnect feature.

### 3 Approach and Implementation

In this section, we integrate PQC accelerators in TaPaSCo. First, we discuss some preliminary considerations. Then, we take the ANSI C reference implementation of CRYSTALS Dilithium and CRYSTALS Kyber as a basis for HLS. Subsequently, we modify the PE interface for Kyber to take a random buffer supplied by the host runtime. Alongside, we outline the key points in the design of the TaPaSCo host runtime application, which is developed to test the designs through the NIST KAT mechanism.

Utilizing the TaPaSCo framework means the functionality of our accelerators is implemented in TaPaSCo Processing Elements (PEs). A PE is a hardware kernel containing the logic to solve a specific task. Usually a TaPaSCo design is composed of multiple PEs, which are accompanied by generic components that are necessary to control their usage such as a Direct Memory Access (DMA) engine, an interrupt controller, and a status core, which stores meta-information about the design that is required by the Linux driver and runtime applications. In this work, we map each operation of a PQC scheme, such as *Encapsulation* or *Sign*, to one PE. First, we need to define an interface to the PEs that minimizes the amount of data necessary to start the PE execution in order to overcome the memory wall. The communication overhead is implementation-independent but an off-chip accelerator should unite most functionality to reduce frequent transfers from and to the general-purpose processor. Most performance evaluations neglect to measure the impact of the communication overhead for off-chip accelerators in a wall clock execution time comparison with the software implementation. For our TaPaSCo PEs, we measure the time necessary to move data from and to the PE and compare it with the optimized AVX2 CPU implementation to set the bottom line for a hardware accelerator. We decide to use the standard NIST interface consisting of `crypto_kem_enc`, `crypto_kem_dec` for KEMs and `crypto_sign`, `crypto_sign_open` for DSAs. This interface has the advantage concerning the memory communication overhead that the parameters, such as keys and ciphertexts, are stored in compressed form, which means it is the smallest data to transfer. Another advantage concerning the host runtime is that all candidates of the NIST PQC project are conforming to this interface, only with different parameter sets. The wrappers around `libtapasco` can leverage Rust's *const generics* feature to be generic over the actually used key sizes. This means if a parameter, like key size, is altered, the change in the runtime implementation is trivial, and extending the runtime application for other parameter sets of other candidates is straightforward. In this work, we use TaPaSCo's HLS interface in the version of commit `1b88fbc` from the `develop` branch, which in turn utilizes the *Xilinx Vitis* toolchain in version `2022.2`. With the use of HLS, we focus on larger high-performance FPGAs because HLS from the software reference implementations is typically inadequate for smaller designs that can fit on IoT-class FPGA devices [5, p. 4]. The FPGA devices used throughout this work are the *Xilinx Virtex-7 VC709* and *Xilinx Alveo U280*. The current ANSI C reference implementation of Dilithium [6, commit `3e9b9f1`] is extended with a TaPaSCo `kernel.json` for each of the top-level functions `crypto_sign` and

`crypto_sign_open` on every security level. We exclude the keypair generation due to its dependence on a secure RNG, which is unavailable on the FPGA. The respective files are located in the `crystals-dilithium` repository in the `kernel` folder ([https://github.com/esa-tu-darmstadt/PQC-HA-CRYSTALS-Dilithium/blob/master/kernel/dilithium2\\_sign/kernel.json](https://github.com/esa-tu-darmstadt/PQC-HA-CRYSTALS-Dilithium/blob/master/kernel/dilithium2_sign/kernel.json)). Apart from meta information such as name, description, and ID, which should be adapted accordingly, only the `CompilerFlags` parameter `DILITHIUM_MODE` is necessary to change the security level. Moving on to CRYSTALS Kyber [4], the software reference implementation [10, commit 518de24] is extended with a TaPaSCo `kernel.json` for each of the top-level functions `crypto_kem_enc` and `crypto_kem_dec` on every security level. The respective files are located in the `crystals-kyber` repository in the `kernel` folder ([https://github.com/esa-tu-darmstadt/PQC-HA-CRYSTALS-Kyber/blob/master/kernel/kyber2\\_enc/kernel.json](https://github.com/esa-tu-darmstadt/PQC-HA-CRYSTALS-Kyber/blob/master/kernel/kyber2_enc/kernel.json)). Note, that the Kyber PEs have the number of the `KYBER_K` parameter in their name, which has the values 2, 3 and 4 but corresponds to NIST security Levels 1, 3, and 5. As for Dilithium, only the `CompilerFlags` parameter `KYBER_K` is necessary to change the security level. It requires only one modification to disable the call to the `randombytes` function for successful HLS compilation. This function fills a buffer with bytes from the Linux RNG, which is necessary to create a secure shared secret and is not available on an FPGA. At this point, the Kyber PEs can generate ciphertexts from which the correct shared secret can be recovered successfully but the buffer usually filled with secure random data in software is left to consist of arbitrary uninitialized memory. Therefore, the random buffer used on the FPGA is initialized from the random data on the host by using the same approach as [16]. The function `crypto_kem_enc` is modified to receive its buffer of random data via a new parameter, thereby moving its declaration into the function signature, while the call to `randombytes` is still disabled. This change is guarded by the `__SYNTHESIS__` conditional compilation mechanism. The runtime expands the `seed` given by the KAT file in the same manner as the official NIST implementation to give the modified *Encapsulation* PE the correctly initialized buffer of random data. With this modification in place, the Kyber *Encapsulation* PE produces the same shared secret and ciphertext as the software implementation and all Kyber PEs are fully verified in hardware. This verification is achieved with the use of KAT response files (suffixed by `.rsp`), generated from the software reference implementation. These can be found directly in the `tapasco-pqc-runtime` repository ([https://github.com/esa-tu-darmstadt/PQC-HA-TaPaSCo-Runtime/blob/main/PQCkemKAT\\_1632.rsp](https://github.com/esa-tu-darmstadt/PQC-HA-TaPaSCo-Runtime/blob/main/PQCkemKAT_1632.rsp)). The runtime first parses the appropriate file for the given algorithm and security level to retrieve a list of usually 100 test cases. The following procedure is the same for both KEMs and DSAs and generic over specific KEMs and DSAs, to be easily extendable when further algorithms will be selected by NIST. The runtime passes the arguments from the test case to the PE associated with the `apply` operation and receives its output, which is passed on to the PE associated with the `verify` operation. The outputs of both PEs are compared with the respective entries in the KAT case and if all entries

match, the test is passed. This process is repeated for every test case in the KAT file.

## 4 Evaluation

In this section, we evaluate the results of the TaPaSCo Design Space Exploration (DSE) in Sect. 4.1. Then, we compare our results with related work using HLS and for an HDL methodology in Sect. 4.2. Finally, we contrast this with a software implementation and analyze the real-world communication overhead from the TaPaSCo host runtime application to the PEs in Sect. 4.3. We implement a bitstream for each PE of Kyber *Encapsulation* and *Decapsulation* and Dilithium *Sign* and *Verify* for all security levels on *Xilinx VC709* and *Alveo U280* FPGAs. All PEs produce correct results, which are verified by the TaPaSCo host runtime application. To measure execution time, the TaPaSCo host runtime application is invoked 1000 times for each PE and software implementation. The VC709 and U280 FPGAs are fully connected over *PCIe 3.0* and the software runs on an *AMD EPYC 743P* CPU. The average of 1000 runs is taken of all runs as in [11]. We report resource utilization of the TaPaSCo *user logic*. This excludes resources required by generic components of every TaPaSCo design, such as the DMA engine, interrupt controller, and status core.

### 4.1 TaPaSCo DSE Results

This section describes the results of the TaPaSCo DSE. In Fig. 1, we plot the resource usage and design frequency of each TaPaSCo Processing Element (TaPaSCo) on the VC709 and U280 platforms. From left to right each PE is shown as a triplet of an algorithm, security level, and operation. The left half displays Kyber, and the right half Dilithium, while security levels are increasing to the right and operations are alternating. The left y-axis shows resource usage as the number of elements, where each color represents another type. DSPs are given in red, BRAMs in green, FFs are given as a multiple of thousand in orange, and LUTs also as a multiple of thousand in blue. The bold black number on top of each bar shows the rounded total sum of the elements used, where LUTs and FFs enter the calculation as thousands. The left bar of each PE represents resource usage on the U280. The right bar shows resource usage on the VC709 platform. BRAMs are given as RAMB36 equivalents, and DSPs as DSP48 for both platforms. The right y-axis shows the design frequency in MHz with a dotted line for U280 and a dashed line for VC709. The resource usage trend across algorithms and operations is identical for both platforms. For both, the number of LUTs, BRAMs, and DSPs is roughly the same, while the number of FFs is consistently higher on VC709. Concerning algorithms, we can see that Kyber uses fewer LUTs, FFs and BRAMs in general, than Dilithium, but required more DSPs. An interesting finding is that, while for Kyber with increasing security level usage of LUTs, FFs and BRAMs declines, the use of DSPs increases, with Kyber 5 *Decapsulation* having the highest usage of DSPs of all. For Dilithium resource

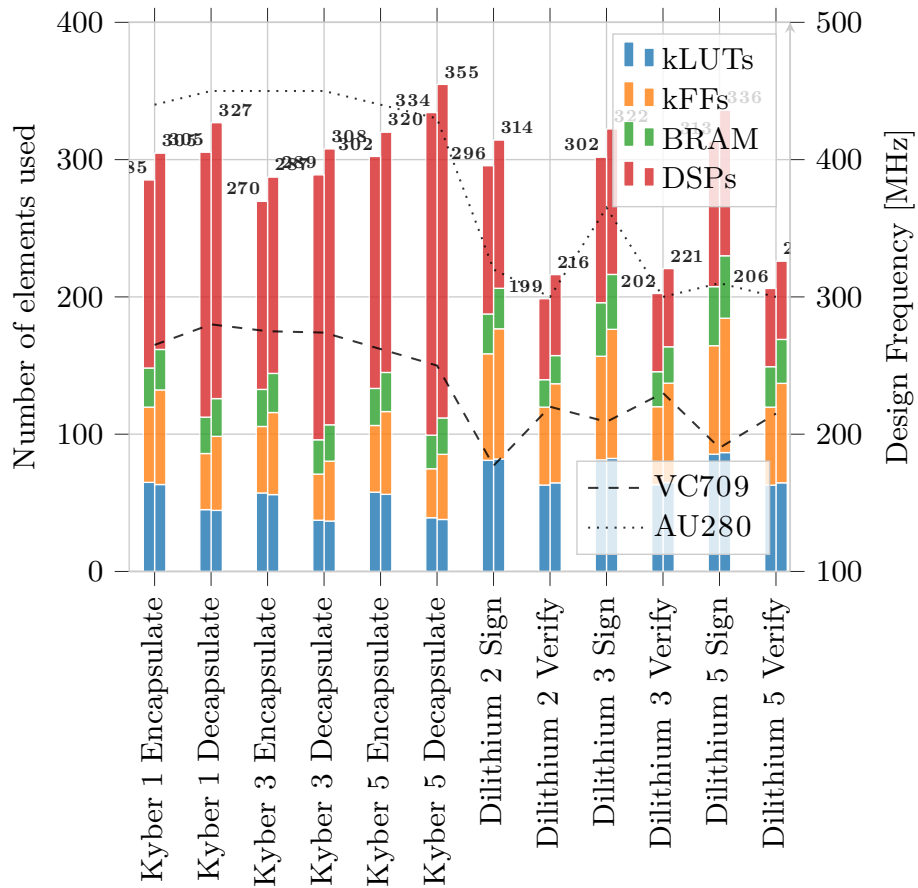


**Fig. 1:** PE Overview of Resource Usage vs. Design Frequency on U280 (left bars) and VC709 (right bars)

usage increases moderately with the security level. With the exception of DSPs of Kyber 5, *Decapsulation* has less resource usage than *Encapsulation* and *Verify* less than *Sign* for Dilithium respectively. Besides using less resources, the U280 reaches almost 1.6 times the design frequency for Kyber and approximately 1.3 times for Dilithium compared to VC709. Kyber achieves higher design frequencies with low variability between different security levels and operations, while for Dilithium on VC709 a clear distinction between *Sign* and *Verify* PEs is visible. On VC709 *Verify* achieves higher frequencies, but on U280 it is *Sign*. In general, we can see that the DSE can yield optima of unexpectedly high frequencies, such as Dilithium 3 *Sign* on U280, but also those lower than usual, that is Dilithium 2 *Sign* on VC709. By utilizing the portability of TaPaSCo designs, moving our PEs to a newer FPGA model can bring less resource usage while achieving higher design frequencies.

## 4.2 Comparison with Related Work

In this section, we compare our TaPaSCo implementations with the results of related work. We first compare the PEs of one scheme with related work that also uses HLS but reports only LUTs and FFs for security Level 1. Then, we compare the PEs of the same scheme with related work that uses an HDL methodology across all security levels. We use the DSE results for VC709 because related work also reports results for Virtex-7 or Artix-7 platforms, whereas the U280 belongs to another generation of FPGAs. We do not apply the Latency-area Product (LAP) as our primary metric because there is no clear methodology how to weight different elements, that is FFs are usually cheaper than DSPs. Therefore we consider resources and latency side-by-side. Additionally, it is unclear how the latency reports are generated in related work. It looks like the hardware execution time is calculated by multiplying latency in the average case with the design frequency, thus not including software overhead. Unfortunately, Vivado does not report the estimated latency of our PEs, which can nevertheless vary a lot due to the algorithmic design of the schemes. The average latency can be analyzed through simulation but for large HLS designs this is slow and for the amount of our PEs therefore infeasible. Instead, we evaluate average execution times in the next section from the software standpoint with the TaPaSCo runtime by measuring the execution time of our PEs including interrupt handling and memory communication overhead.

In Fig. 2, we compare our Kyber and Dilithium PEs of security Level 1 on VC709 with the results of related work in [1] on VC707 and [16] as well as [1] on VC709. We only compare LUTs and FFs because the authors of related work do not report their utilization of BRAMs and DSPs. From left to right, each implementation is displayed as a combination of work/author, optimization level, and operation, where *Encapsulation* is compared in the first third, *Decapsulation* in the second third and *Sign* and *Verify* in the last third. The left y-axis shows the number of elements used, where LUTs and FFs are given as multiple of thousand in blue and orange respectively. The right y-axis shows the mean execution time measured in software for this work and calculated from latency and frequency



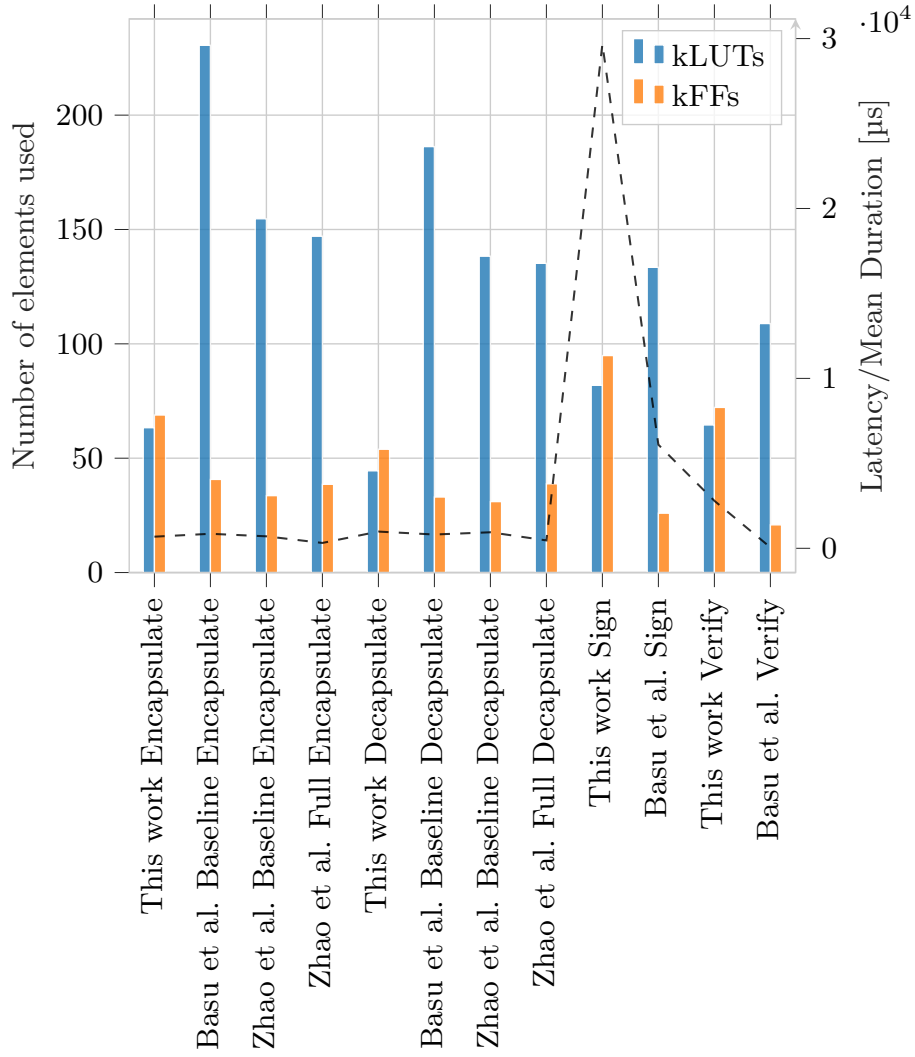


**Fig. 2:** Comparison of TaPaSCo Kyber and Dilithium PEs on Virtex-7 and Security Level 1 with related work using an HLS approach

for related work in micro-seconds as a dashed line. For Kyber, we observe that our designs use the least LUTs and the most FFs for both operations, with the lowest resource utilization in total. The reduced usage of LUTs probably incurs the cost of more DSPs but related work does not report numbers for their use of this element. However, while the latency for *Encapsulation* is at the same level as the baseline implementation from Zhao *et al.* and better than the baseline implementation of Basu *et al.*, the latency for *Decapsulation* is higher than those of all other implementations. However, their latency report does not include overhead contained in the result for TaPaSCo PEs. Employing the same optimizations as Zhao *et al.* would be interesting but is not promising when compared to related work using an HDL approach as seen in Fig. 4.

For Dilithium, we observe that our PEs use fewer LUTs and more FFs than the implementations of Basu *et al.* leading to a higher resource utilization overall. To conclude, this means that our HLS approach with minimally modified C code is more suited for Kyber than Dilithium to produce low resource utilization with comparable latency but in general yields decent results compared to other HLS-based works.

In Fig. 3, we compare our Kyber PEs on all security levels with the results of related work in [5]. From left to right, each PE is shown as a triplet of work/author, operation, and security level. The left half displays our Kyber PEs and the right half the implementations from Dang, Mohajerani, and Gaj, while security levels are increasing to the right and operations are alternating. The left y-axis shows resource usage as the number of elements in a logarithmic scale, where each color represents another type. LUTs are given as a multiple of thousand in blue, FFs also as a multiple of thousand in orange, BRAMs in green and DSPs are given in red. The right y-axis shows the mean execution time measured in software for this work and calculated from latency and frequency for related work in micro-seconds as a dashed line in a logarithmic scale. This diagram affirms the conclusion of Dang, Mohajerani, and Gaj that HLS implementations cannot keep up with HDL designs. Our PEs have roughly a magnitude higher resource utilization, even though they are specialized for each operation and their core is capable of both operations and key generation for each security level. Finally, their latency/mean execution time is also more than a magnitude lower but this still does not yield enough performance to overcome the memory wall as we show in the next section.

In Fig. 4, we compare our Dilithium PEs on all security levels with the results of related work in [11]. From left to right, each PE is shown as a triplet of work/author, operation, and security level. The left half displays our Dilithium PEs and the right half the implementations from Land, Sasdrich, and Güneysu, while security levels are increasing to the right and the *Sign* operation is shown first, Verification second. The y-axis shows resource usage and mean execution time as in the last diagram Fig. 3. This diagram confirms the conclusion of Dang, Mohajerani, and Gaj that HLS implementations cannot keep up with HDL designs for Dilithium too. Our PEs have roughly a magnitude higher resource utilization, even though they are specialized for each operation and their core is capable of both operations and key generation. Finally, their latency/mean

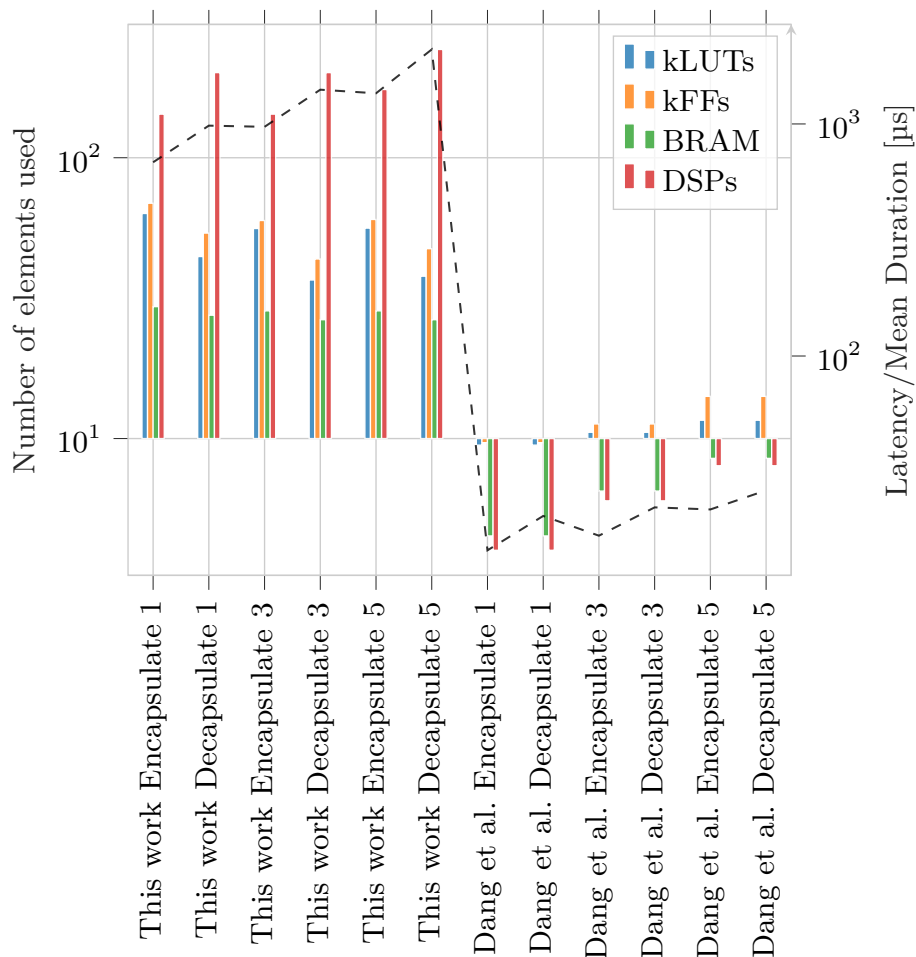


**Fig. 3:** Comparison of TaPaSCo Kyber PEs on Virtex-7 and related work from Dang et al. (HDL) on Artix-7

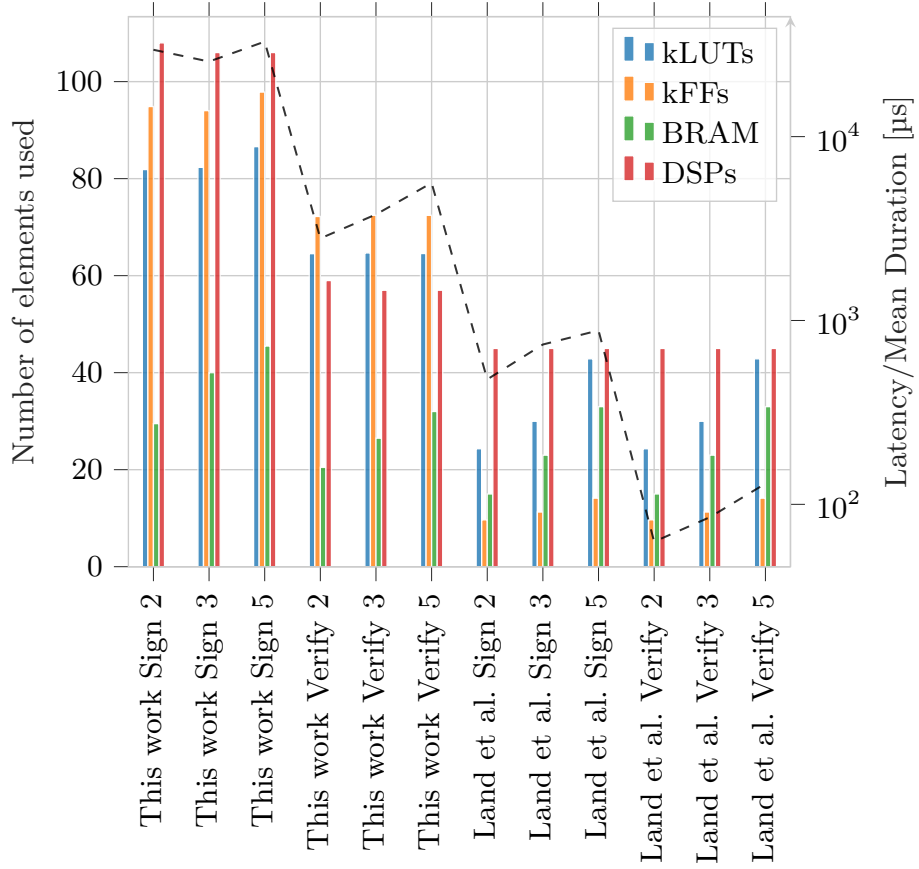


**Fig. 4:** Comparison of TaPaSCo Dilithium PEs on Virtex-7 and related work from Land et al. (HDL) on Artix-7

execution time is also more than a magnitude lower. Yet, this does not yield enough performance to compete with the optimized Advanced Vector Extensions 2 (AVX2) implementation, as we will see in the next section.

### 4.3 Comparison of Execution Time against Software

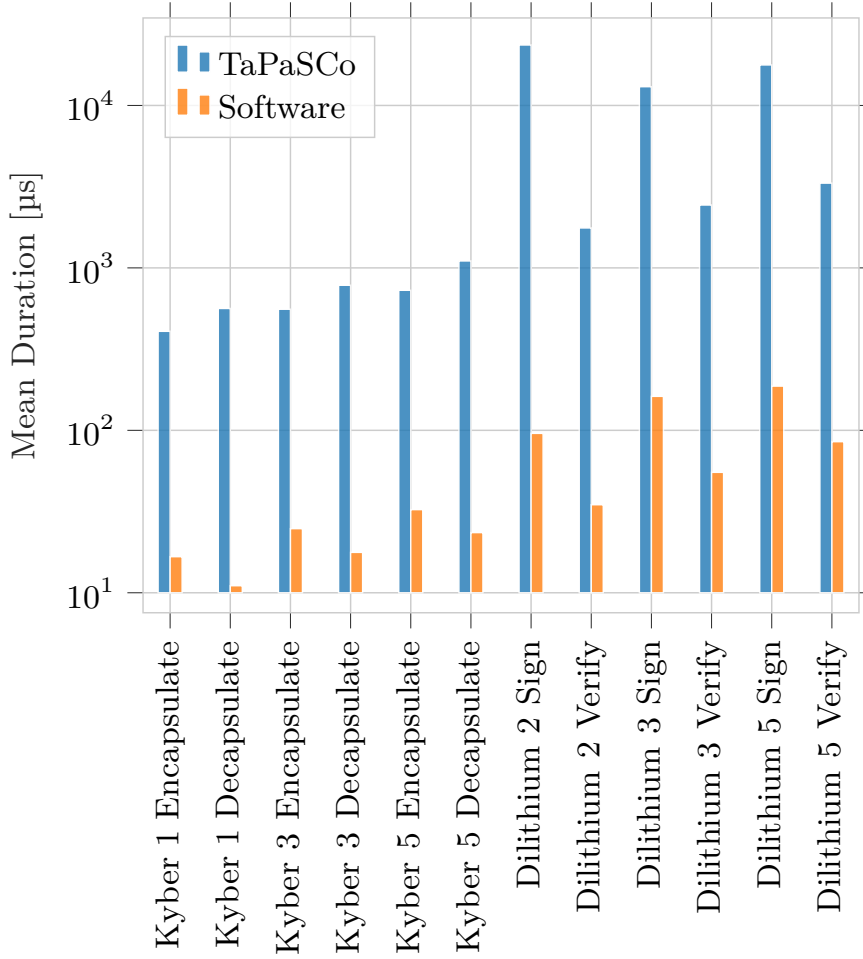


**Fig. 5:** Mean Execution Time of TaPaSCo on U280 and AVX2 Software Implementation on AMD Epyc

In this section, we compare our results against the software implementations of Kyber and Dilithium. As TaPaSCo PEs are standalone accelerators, we evaluate the communication overhead introduced by the host and FPGA memories

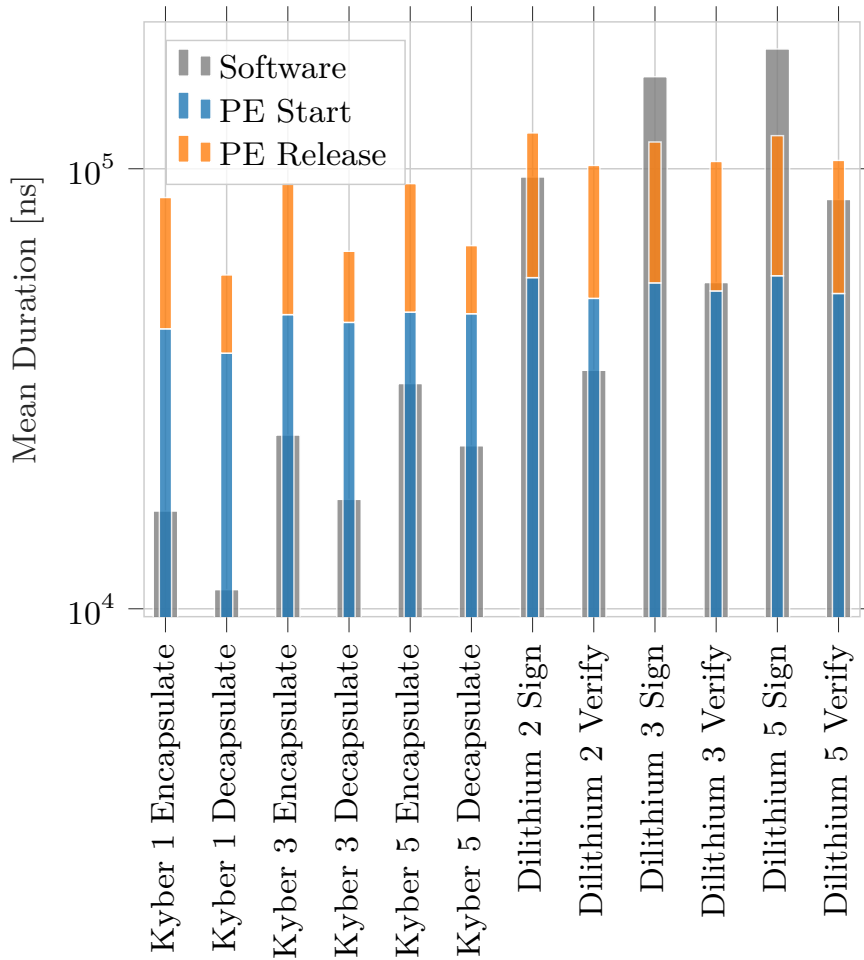


**Fig. 6:** Communication Overhead of TaPaSCo on U280 and Mean Execution Time in AVX2 Software Implementation on AMD Epyc

connected through *Peripheral Component Interconnect Express (PCIe) 3.0*. We test under realistic conditions from the same application on the same host and also include software interrupt handling overhead.

In Fig. 5, we compare the execution time from the TaPaSCo host runtime application with the optimized AVX2 implementation running on the host Central Processing Unit (CPU). From left to right, all our implementations are listed as triplets of the algorithm, security level, and the operation. The left half shows results for Kyber, the right half for Dilithium. The y-axis shows the mean execution time in micro-seconds on a logarithmic scale of both TaPaSCo in blue bars and the AVX2 software implementation in orange bars. We observe that the software implementation is roughly one magnitude faster than the TaPaSCo PEs.

In Fig. 6, we compare the communication overhead of the TaPaSCo host runtime application with the optimized AVX2 Implementation running on the host CPU. From left to right, all our implementations are listed as a triplet of algorithm, security level, and operation. The left half shows results for Kyber, the right half for Dilithium. The y-axis shows the mean execution time in nano-seconds on a linear scale of the AVX2 software implementation in gray bars and the communication overhead for preparation of a PE as blue and the release of a PE as orange bar stacked on top of each other. Across all PEs, the communication overhead is around/less than 10 000 ns. Mean execution time in software increases generally with security level, while for Kyber both operations have roughly the same value with *Decapsulation* only slightly lower than *Encapsulation*, Dilithium varies greatly between signing and verification. We observe that for Kyber 1 *Encapsulation* the communication overhead alone is almost as high as the effort to solve the original problem itself. For Kyber 1 *Decapsulation* the communication overhead alone is already higher than the software implementation. For Kyber 3 the overhead takes up half of the software implementation and for Kyber 5 approximately a third. We conclude that using the TaPaSCo architecture accelerating Kyber on security Level 1 is impossible on the evaluated platform and even using the state-of-the-art HDL accelerator from Dang, Mohajerani, and Gaj would not be faster than the AVX2 software implementation. The same holds for the Dilithium implementation from Land, Sasdrich, and Güneysu, assuming the same communication overhead for their interface when integrated into the TaPaSCo architecture. However, this only holds true if the only metric employed is latency. The obvious next step to evaluate throughput on *high-performance* FPGA devices is to look at *pipelining*. Other scaling mechanisms such as using multiple PEs concurrently in a cluster are also possible and can be combined with multi-potent HDL designs, where each PE can perform all operations of the scheme, e. g., key generation, encapsulation, and decapsulation for a KEM, and executes the desired operation according to the current demand. Accumulating multiple outstanding memory requests could also result in a benefit concerning the communication overhead and lower overhead could in turn increase throughput again. Finally, regarding these results

for high-performance standalone accelerators, it would be interesting to see more in-pipeline accelerators like those of [7] but for *high-performance* CPUs.

## 5 Conclusion

We integrated the software implementations of two algorithms from the NIST PQC project into a generic FPGA runtime utilizing the features of TaPaSCo via HLS. We present a bitstream for CRYSTALS Kyber and Dilithium on all three security levels for *Encapsulation/Sign* and *Decapsulation/Verify*. Our approach leads to designs with comparable resource utilization and performance to baseline results of related work also using HLS while achieving a higher design frequency as a result of the TaPaSCo DSE. They are verified in hardware to produce the same correct results as the software implementation through the KAT mechanism. This straightforward methodology is adequate to develop a TaPaSCo host runtime application and evaluate the PE interface including the corresponding communication overhead but is clearly inferior in terms of resource utilization and performance compared to HDL designs of related work. We demonstrate portability by synthesizing the same designs for VC709 and U280, thereby gaining faster designs while lowering resource utilization. We analyze the communication overhead for standalone memory-mapped accelerators and conclude that by utilizing the TaPaSCo PE architecture, there is only a tight window for speeding up Kyber against the optimized reference AVX2 implementation. For Kyber on security Level 1, the communication overhead is even as high as the time necessary to solve the operation in software. The window for Dilithium is larger, especially for the Sign operation, but assuming the same overhead, it is questionable if even state-of-the-art HDL implementations could beat the optimized software implementation in the high-performance domain. To wrap up, TaPaSCo can aid with the design process by using its PE architecture and shines in testing of PQC accelerators on real hardware utilizing its Linux kernel driver and our generic runtime. For the NIST PQC project specifically, the ANSI C reference implementations are straightforward to integrate into the TaPaSCo ecosystem via HLS but this does not replace the HDL methodology.

## 6 Future Work

With the foundation for TaPaSCo PQC accelerators laid in this work, there are multiple promising ways for further exploration. First, existing hardware implementations that are published as open-source can be integrated in the TaPaSCo PE architecture, where lightweight designs open the possibility to make use of the diverse TaPaSCo device support for smaller FPGAs. There, the communication overhead can be re-evaluated on embedded platforms that use a different memory architecture, such as shared memory on the Ultra96, and compared to the optimized software implementations of other CPU Instruction Set Architectures (ISAs), e. g., Neon NTT [2] on ARM. Finally, the HLS-based TaPaSCo approach as shown in this work can be applied to other, more unexplored,



alternate candidates of the NIST PQC project for the next round, where all TaPaSCo components, including the host runtime application can be re-used because all candidates are required to conform to the same interface.

## References

1. Basu, K., Soni, D., Nabeel, M., Karri, R.: NIST Post-Quantum Cryptography – A Hardware Evaluation Study. 047, (2019). <http://eprint.iacr.org/2019/047> (visited on 05/06/2021)
2. Becker, H., Hwang, V., Kannwischer, M.J., Yang, B.-Y., Yang, S.-Y.: Neon NTT: Faster Dilithium, Kyber, and Saber on Cortex-A72 and Apple M1. 986, (2021). <http://eprint.iacr.org/2021/986> (visited on 10/21/2021)
3. Beckwith, L., Nguyen, D.T., Gaj, K.: High-Performance Hardware Implementation of CRYSTALS-Dilithium. 1451, (2021). <http://eprint.iacr.org/2021/1451> (visited on 11/17/2021)
4. Bos, J., Ducas, L., Kiltz, E., Lepoint, T., Lyubashevsky, V., Schanck, J.M., Schwabe, P., Seiler, G., Stehlé, D.: CRYSTALS – Kyber: a CCA-secure module-lattice-based KEM. 634, (2017). <http://eprint.iacr.org/2017/634> (visited on 05/06/2021)
5. Dang, V.B., Mohajerani, K., Gaj, K.: High-Speed Hardware Architectures and FPGA Benchmarking of CRYSTALS-Kyber, NTRU, and Saber. 1508, (2021). <http://eprint.iacr.org/2021/1508> (visited on 11/27/2021)
6. Dilithium, (2021). <https://github.com/pq-crystals/dilithium> (visited on 11/27/2021)
7. Fritzmann, T., Sigl, G., Sepúlveda, J.: RISQ-V: Tightly Coupled RISC-V Accelerators for Post-Quantum Cryptography. 446, (2020). <http://eprint.iacr.org/2020/446> (visited on 06/01/2021)
8. Heinz, C., Hofmann, J., Korinth, J., Sommer, L., Weber, L., Koch, A.: The TaPaSCo Open-Source Toolflow: for the Automated Composition of Task-Based Parallel Reconfigurable Computing Systems. *J Sign Process Syst* (2021). <https://doi.org/10.1007/s11265-021-01640-8>. <https://link.springer.com/10.1007/s11265-021-01640-8> (visited on 05/11/2021)
9. Heinz, C., Lavan, Y., Hofmann, J., Koch, A.: A Catalog and In-Hardware Evaluation of Open-Source Drop-In Compatible RISC-V Softcore Processors. In: 2019 International Conference on ReConFigurable Computing and FPGAs (ReConFig), pp. 1–8. IEEE, Cancun, Mexico (2019). <https://doi.org/10.1109/ReConFig48160.2019.8994796>. <https://ieeexplore.ieee.org/document/8994796/> (visited on 11/24/2021)
10. Kyber, (2021). <https://github.com/pq-crystals/kyber> (visited on 11/27/2021)
11. Land, G., Sasdrich, P., Güneysu, T.: A Hard Crystal - Implementing Dilithium on Reconfigurable Hardware. 355, (2021). <http://eprint.iacr.org/2021/355> (visited on 05/07/2021)
12. Ricci, S., Malina, L., Jedlicka, P., Smekal, D., Hajny, J., Cibik, P., Dobias, P.: Implementing CRYSTALS-Dilithium Signature Scheme on FPGAs. 108, (2021). <http://eprint.iacr.org/2021/108> (visited on 05/07/2021)
13. Soni, D.: deepraj88 - Overview. GitHub, <https://github.com/deepraj88> (visited on 11/27/2021)
14. Soni, D.: NIST Round 2 PQCs: FPGA Implementations – Hardware Assessment of NIST Post Quantum Crypto, [https://wp.nyu.edu/hipqccheck/round2\\_implementation/](https://wp.nyu.edu/hipqccheck/round2_implementation/) (visited on 11/27/2021)

15. Soni, D., Basu, K., Nabeel, M., Aaraj, N., Manzano, M., Karri, R.: Hardware Architectures for Post-Quantum Digital Signature Schemes. Springer International Publishing, Cham (2021)
16. Zhao, Y., Chao, Z., Ye, J., Wang, W., Cao, Y., Chen, S., Li, X., Li, H.: Optimization Space Exploration of Hardware Design for CRYSTALS-KYBER. In: 2020 IEEE 29th Asian Test Symposium (ATS), pp. 1–6 (2020). <https://doi.org/10.1109/ATS49688.2020.9301498>. <https://ieeexplore.ieee.org/document/9301498> (visited on 12/02/2021)

Table 1: List of all PEs with design frequency and resource utilization

Algorithm	Platform	Security Level	Operation	PE Name	Functionality	Frequency [MHz]	kLUTs	kFPs	BRAM	DSPs
0	Kyber									
1	VC709	1	Encapsulate	kyber2_enc	Working	265	63,329,000	68,883,000	29,500,000	143,000,000
2	Kyber	1	Decapsulate	kyber2_dec	Working	280	44,488,000	53,918,000	27,500,000	201,000,000
3	VC709	3	Encapsulate	kyber3_enc	Working	275	55,982,000	59,783,000	28,500,000	143,000,000
4	Kyber	3	Decapsulate	kyber3_dec	Working	274	36,704,000	43,616,000	26,500,000	201,000,000
5	VC709	5	Encapsulate	kyber4_enc	Working	262	56,166,000	60,297,000	28,500,000	175,000,000
6	Kyber	5	Decapsulate	kyber4_dec	Working	250	37,864,000	47,445,000	26,500,000	243,000,000
7	Kyber	1	Encapsulate	kyber2_enc	Working	440	64,900,000	54,792,000	26,500,000	137,000,000
8	AU280	1	Decapsulate	kyber2_dec	Working	450	45,038,000	40,858,000	26,500,000	193,000,000
9	Kyber	3	Encapsulate	kyber3_enc	Working	450	57,164,000	48,447,000	27,000,000	137,000,000
10	AU280	3	Decapsulate	kyber3_dec	Working	450	37,307,000	33,600,000	25,000,000	193,000,000
11	Kyber	5	Encapsulate	kyber4_enc	Working	440	57,745,000	48,585,000	27,000,000	169,000,000
12	AU280	5	Decapsulate	kyber4_dec	Working	430	39,127,000	35,664,000	24,500,000	285,000,000
13	Dilithium	2	Sign	dilithium2_sign	Deadlock	177	81,877,000	94,875,000	29,500,000	108,000,000
14	VC709	2	Verify	dilithium2_verify	Working	220	64,537,000	72,207,000	20,500,000	59,000,000
15	Dilithium	3	Sign	dilithium3_sign	Working	209	82,336,000	94,028,000	40,000,000	106,000,000
16	VC709	3	Verify	dilithium3_verify	Working	230	64,691,000	72,448,000	26,500,000	57,000,000
17	Dilithium	5	Sign	dilithium5_sign	Working	190	86,601,000	97,852,000	45,500,000	106,000,000
18	VC709	5	Verify	dilithium5_verify	Working	215	64,569,000	72,445,000	32,000,000	57,000,000
19	Dilithium	2	Sign	dilithium2_sign	Deadlock	320	80,943,000	77,604,000	29,000,000	108,000,000
20	AU280	2	Verify	dilithium2_verify	Working	300	62,922,000	56,764,000	20,000,000	59,000,000
21	Dilithium	3	Sign	dilithium3_sign	Working	365	81,262,000	75,504,000	39,000,000	106,000,000
22	AU280	3	Verify	dilithium3_verify	Working	300	63,204,000	56,795,000	25,500,000	57,000,000
23	Dilithium	5	Sign	dilithium5_sign	Working	310	85,421,000	79,031,000	43,000,000	106,000,000
24	AU280	5	Verify	dilithium5_verify	Working	300	62,857,000	56,795,000	29,500,000	57,000,000

**Table 2:** List of all PEs with mean execution time and communication overhead

Algorithm	Platform	Security Level	Operation	PE Name	Functionality	Frequency [MHz]	PE Start [ns]	PE Wait [ns]	PE Release [ns]	Mean Duration [ $\mu$ s]
0	Kyber		Encapsulate	kyber2_enc	Working	265	33 879 021 000	625 722 209 000	24 261 589 000	683 862 819
1	Kyber	1	Decapsulate	kyber2_dec	Working	280	38 860 905 000	927 236 989 000	17 254 458 000	983 352 352
2	Kyber	3	Encapsulate	kyber3_enc	Working	275	39 136 417 000	908 713 685 000	23 993 971 000	971 844 073
3	Kyber	3	Decapsulate	kyber3_dec	Working	275	36 845 543 000	1 353 062 283 000	14 922 066 000	1 404 829 892
4	Kyber	5	Encapsulate	kyber4_enc	Working	262	33 415 510 000	1 300 124 540 000	21 841 251 000	1 355 381 301
5	Kyber	5	Decapsulate	kyber4_dec	Working	250	40 440 257 000	2 036 665 064 000	16 949 798 000	2 094 055 119
6	Kyber	1	Encapsulate	kyber2_enc	Working	440	43 271 507 000	320 937 785 000	42 768 400 000	407 008 656
7	Kyber	1	Decapsulate	kyber2_dec	Working	450	38 101 868 000	505 237 785 000	19 285 876 000	562 625 529
8	Kyber	3	Encapsulate	kyber3_enc	Working	450	46 614 493 000	463 630 703 000	46 358 170 000	556 603 366
9	Kyber	3	Decapsulate	kyber3_dec	Working	450	44 759 069 000	717 163 692 000	20 182 781 000	782 105 542
10	Kyber	5	Encapsulate	kyber4_enc	Working	440	46 826 185 000	1 036 884 439 000	45 309 562 000	728 079 743
11	Kyber	5	Decapsulate	kyber4_dec	Working	430	47 224 161 000	635 546 020 000	20 067 314 000	1103 777 938
12	Dilithium	2	Sign	dilithium2_sign	Deadlock	177	49 764 878 000	29 582 405 304 000	43 248 174 000	29 675 418 265
13	Dilithium	2	Verify	dilithium2_verify	Working	220	37 304 096 000	2 728 635 281 000	29 307 401 000	25 602 066 243
14	Dilithium	3	Sign	dilithium3_sign	Working	209	45 676 437 000	25 517 599 169 000	38 890 637 000	27 952 246 778
15	Dilithium	3	Verify	dilithium3_verify	Working	230	40 676 837 000	3 705 498 223 000	27 473 324 000	32 858 855 607
16	Dilithium	5	Sign	dilithium5_sign	Working	190	44 947 777 000	33 771 644 154 000	42 263 676 000	55 999 710 570
17	Dilithium	5	Verify	dilithium5_verify	Working	215	40 420 255 000	5 532 179 893 000	27 110 452 000	23 564 663 024
18	Dilithium	2	Sign	dilithium2_sign	Deadlock	320	56 567 794 000	23 444 002 396 000	64 092 834 000	1 762 056 637
19	Dilithium	2	Verify	dilithium2_verify	Working	300	50 028 980 000	1 660 295 248 000	51 009 036 000	13 047 174 279
20	Dilithium	3	Sign	dilithium3_sign	Working	365	52 756 371 000	2 384 493 162 000	60 011 130 000	2 438 392 369
21	Dilithium	3	Verify	dilithium3_verify	Working	300	57 123 034 000	17 644 266 313 000	61 795 863 000	17 763 185 210
22	Dilithium	5	Sign	dilithium5_sign	Working	310	52 060 355 000	3 220 930 649 000	52 414 143 000	3 325 405 147
23	Dilithium	5	Verify	dilithium5_verify	Working	300				